Morphological characterization of compact aggregates using image analysis and a geometrical stochastic 3D model

Léo Théodon, Carole Coufort-Saudejaud, Ali Hamieh, Johan Debayle

Morphological characterization of compact aggregates using image analysis and a geometrical stochastic 3D model

Léo Théodon
CNRS, UMR 5307 LGF, Centre SPIN
MINES Saint-Etienne
Saint-Etienne, France
l.theodon@emse.fr

Carole Coufort-Saudejaud
Laboratoire de Génie Chimique
Université de Toulouse
CNRS, INPT, UPS, Toulouse, France
carole.saudejaud@toulouse-inp.fr

Ali Hamieh
Laboratoire de Génie Chimique
Université de Toulouse
CNRS, INPT, UPS, Toulouse, France
TBI, Université de Toulouse
CNRS, INRAE, INSA
Toulouse, France
ali.hamieh@toulouse-inp.fr

Johan Debayle
CNRS, UMR 5307 LGF, Centre SPIN
MINES Saint-Etienne
Saint-Etienne, France
debayle@emse.fr

***Abstract*—The 3D morphological characteristics of size and shape of latex nanoparticle aggregates have a major impact on the quality of these powders and their performances such as flowability/processability in an industrial context. Most of the time the morphological characterization of these aggregates is only possible from the analysis of projected images, which only allows to measure 2D features. In this paper, a method for the 3D morphological characterization of a compact aggregate from the analysis of a single image is proposed. This method is composed of three steps: the description of a stochastic geometric model, the acquisition of data from image analysis, and the fitting of the model parameters to the data using an optimization process. The method was validated using images of a calibrated 3D printed aggregate, and the results presented in the last section show discrepancies lower than 1% for 2D morphological characteristics and lower than 2% in most cases for 3D characteristics. The limitations of the model are discussed and suggestions for improvement are made in the conclusion.**

***Index Terms*—Aggregates, Digital twins, Geometric modeling, Image analysis, Modeling, Simulation, Stochastic geometry**

I. Introduction

The morphological characterization of particle aggregates by image analysis is a common problem in many scientific fields such as the chemical industry [1, 2], the medical field [3, 4], the food industry [5–9] or civil engineering [10]. Depending on the characteristics studied and the type of aggregate, different techniques can be used: SEM [11], X-Ray CT images [10], video capture [12], multiple cameras [13] or multiple point of view [14]. More generally, the morphological characterization of an object such as an aggregate can have a different meaning depending on the context. Indeed, several types of morphological characteristics can be distinguished, such as the characteristics of shape, size or texture [15] and, therefore, the physical characteristics such as the mass and chemical characteristics are generally excluded.

The most commonly calculated size characteristic is the Particle Size Density (PSD), which corresponds to the size density of each of the aggregates, and, when possible, the primary particle density, which corresponds to the size density of each of the primary particles of the aggregates. To this end, recent machine learning techniques allowing the segmentation of aggregates of particles of varying sizes have been successfully developed [16–19]. Regarding the shape characteristics, such as the elongation, the fractality or the porosity, these are particularly used to describe crystalline [3–5, 14] aggregates or coarse aggregates [10].

When it comes to characterizing aggregates by image analysis, two main categories of techniques exist. Direct methods propose to perform measurements directly on the images, using advanced image processing techniques [1, 20]. These methods are particularly effective when the images are of good quality, i.e. the shapes are easy to binarize and to isolate from each other. On the other hand, they become complex to implement when the number of objects to characterize is important or when they overlap. In this case, the use of indirect methods, such as stochastic methods based on models, can be very powerful [10, 11, 21–23]. The idea is then to model the aggregation phenomenon and to generate synthetic images with the same average characteristics as the real images. When there is a match, the characteristics of the real objects are known through the characteristics of the synthetic objects generated by the model.

II. Overview & Methodology

The aim of this paper is to propose a method for the characterization of compact nanoparticle aggregates by image analysis and stochastic geometry. The problem at hand is the morphological characterization of a latex nanoparticle aggregate. This aggregate is the constituent of a powder whose grain size and shape has a considerable influence on the efficiency of the industrial processes in which it is used. The main goal is then the 3D morphological characterization of an aggregate of particles from a single 2D image. The 3D characterization of an aggregate from several images is a problem that has already been studied [6, 10], but the 3D characterization of an object from even multiple 2D measurements remains difficult [24]. Therefore, the proposed method is original because it allows to fully describe the 2D and 3D morphology of a particle aggregate when only one image is available by combining direct image analysis techniques with the use of a stochastic geometrical model.

The proposed method consists of three steps.

1) BLOSSOM[1], a geometric stochastic parametric model for generating synthetic 3D aggregates of spherical particles of same size, is defined.
2) An aggregate image is analyzed and 2D morphological characteristics are measured. Image analysis is also used to calibrate certain parameters of the BLOSSOM model.
3) A cost function is defined and its optimization allows to determine an optimal set of parameters for the BLOSSOM model. With this optimal set of parameters, the synthetic aggregates have the same 2D morphological characteristics as those measured on the original image. This leads to the conclusion that the 3D morphological characteristics are also identical.

In the following section, the 2D and 3D morphological characteristics that will be measured and used throughout this paper are defined. The BLOSSOM model is then defined, and example implementations with different sets of parameters are presented. The fitting of the model to real data using image analysis is then described. In particular, a 3D printed aggregate of quasi-spherical particles is used to validate the method. Images of this aggregate were taken with a morphogranulometer (Morphologi G3 – Malvern Panalytical) and the 3D morphological characteristics of the 3D printed aggregate are known thanks to a reference STL file. It is worth mentioning that the 3D printed aggregate strongly resembles the latex nanoparticle aggregates mentioned in the previous section. The results of the optimization are presented and explained in the last section. In particular, the 3D characteristics predicted by the BLOSSOM model are compared to those contained in the STL file. Finally, the limitations of the model are discussed and possible improvements are suggested.

III. Morphological characterization

In this section, the 2D and 3D morphological properties that will be used to characterize particle aggregates are defined.

[1]BLossoming Overlapping Spheres Self-Organizing Model

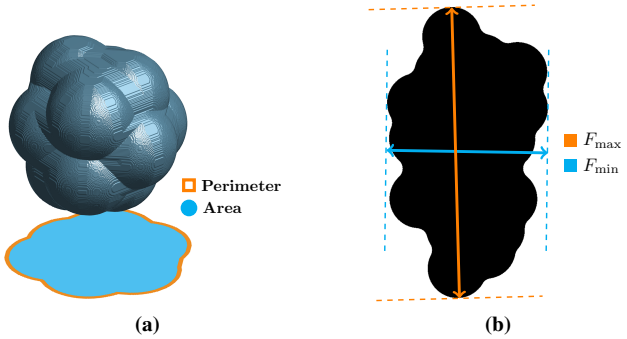

Fig. 1: (a) Illustration of the projected area (blue) and perimeter (red) of an aggregate. (b) Illustration of the calculation of the maximum and minimum Feret diameters.

a) Aspect ratio: The aspect ratio Ψ_{AR} is defined as the ratio of the minimum and maximum Feret diameters.

$$\Psi_{AR} = F_{\min}/F_{\max} \in [0;1]. \tag{1}$$

b) Projected area and perimeter: The projected area and perimeter are usually measured on binary images of an aggregate projection along an axis. Depending on the 3D morphology of the aggregate and the axis considered, these characteristics can change significantly (Fig. 1a).

c) Feret diameters: The Feret diameters of a binary shape correspond to the distance between two parallel lines arranged in such a way that the shape is located exactly between these two lines. The maximum (resp. minimum) Feret diameter corresponds to the maximum (resp. minimum) possible distance between these two lines (Fig. 1b).

d) Centroid: The centroid of a binary shape is the point corresponding to the center of mass of the pixels (or voxels in 3D) belonging to the shape.

e) Volume: The volume of an aggregate V is usually calculated by summing a number of voxels of a 3D binary shape in a discrete space.

f) Convex volume: The convex volume V_c is the volume of the convex envelope of a 3D shape.

g) Solidity and porosity: The solidity SLD $\in [0;1]$ is the ratio of the volume V over the convex volume V_c.

$$\text{SLD} = V/V_c. \tag{2}$$

Low strength may indicate high porosity ϕ of the aggregate, the latter being defined as follows.

$$\phi = V_{\text{pores}}/V. \tag{3}$$

h) Surface area: The surface area S is the closed surface of a 3D shape.

i) Equivalent diameter: The equivalent diameter or equivalent spherical diameter (ESD) is the diameter of a sphere having the same volume as the considered 3D shape.

$$\text{ESD} = \sqrt[3]{\frac{6 \times V}{\pi}} \tag{4}$$

j) Principal axis length: The principal axis length (PAL) correspond to the length of the three major axes of the ellipsoid having the same co-variance matrix as the voxels representing the considered 3D binary shape.

IV. Stochastic model

A. Model definition

The generation of an aggregate by the BLOSSOM model corresponds to an iterative process. At each iteration, a hard sphere is added to the aggregate being generated. A parameter d_α allows a certain overlap distance between the spheres. This process can be described as follows.

1) A spherical particle is created at coordinates $(0; 0; 0)$. During the whole process, if the particle is not in contact with another particle (according to d_α, the overlap parameter), it stands still and the next iteration is performed.
2) A direction vector $\vec{v} = (\Delta\rho, \theta, \varphi)$ is drawn at random, and the particle will then move along this direction, the displacement step depending on the parameter $\Delta\rho$. The probability density functions related to φ and θ are respectively f_φ and f_θ.
3) When the current particle stops moving, and if the maximum number of particles N_p has been reached, the process stops. Otherwise, a new particle is created, and the process goes to the next iteration.

The BLOSSOM model depends on 4 numerical parameters (Tab. I) and 2 probability density functions to express the random coordinates of the vector $\vec{v}$ determining the direction of the moving particle at each iteration. These coordinates are expressed in spherical coordinates. Regarding the overlap parameter d_α, it is expressed as a ratio of the diameter of the particles. Thus, $d_\alpha = 0$ indicates that only single point contacts are allowed, while a ratio of $d_\alpha = 0.5$ authorizes an overlap of 50% of the diameter, i.e. of the radius r of the particles.

TABLE I: Listing of the BLOSSOM model parameters.

Parameters	**Definition**
N_p	Number of particles
r	Radius of the particles
d_α	Overlap parameter
$\Delta\rho$	Displacement step
f_θ, f_φ	Probability density functions

In order to ensure that each particle has at least one point of contact with the aggregate being generated, a reassembly operation is performed at the end of each iteration. In addition, a repulsive force of low intensity relative to the displacement step is added to the aggregate being generated, so that the mobile particle finds an available location more quickly. This also prevents the aggregates from being too porous in the case of a high displacement step. More precisely, in case of an overlap greater than d_α, the mobile particle is repelled according to a vector $\vec{u}$ in a direction orthogonal to the vector $\vec{v}$, and whose modulus is a fraction of $\Delta\rho$, proportional to the overlap.

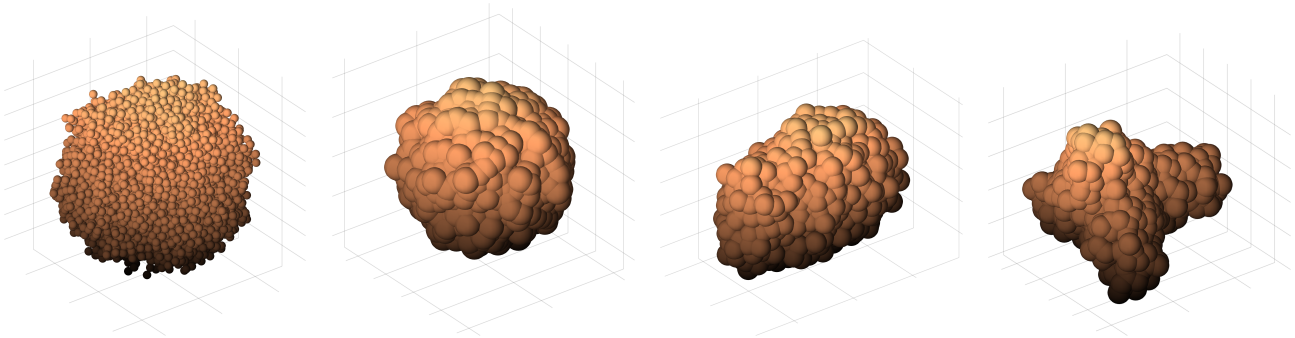

Fig. 2: Examples of aggregates generated by the BLOSSOM model with, from left to right, a number of particles $N_p = \{5000, 1500, 1000, 1000\}$, an overlap parameter $d_\alpha = \{0, 0.75, 0.5, 0.6\}$, and density probability functions f_θ and f_φ displayed on Fig. 3. The parameters r and Δ_ρ are constant.

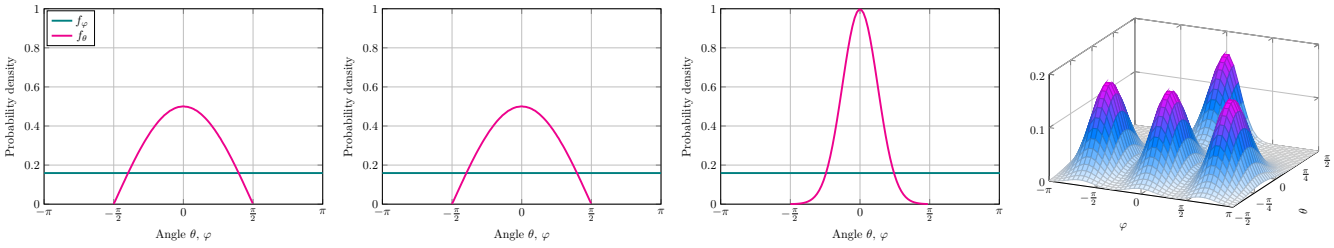

Fig. 3: Probability density functions used to generate the aggregates in Figure 2. The probability densities allow a uniform distribution on the sphere for the first two aggregates, and f_θ is a von Mises distribution [25] for the third aggregate while f_φ and f_θ are a joint mixture of four normal distributions for the fourth one.

B. Example of realizations

Figure 2 shows some examples of realizations of the BLOSSOM model using different sets of parameters. The overlap parameter d_α has a direct impact on many morphological characteristics of the aggregates, such as porosity ϕ, solidity SLD or surface area S. The probability density functions f_θ and f_φ (Fig. 3), and, not surprisingly, the number of particles N_p, have an significant impact on the shape and size of the aggregate.

In particular, if f_θ and f_φ are constant, the aggregates are rather spherical and as long as f_φ remains constant, the aggregates have some cylindrical symmetry. Joint distributions for f_θ and f_φ allow to generate more complex aggregates with concavity and lower solidity SLD. Finally, a large overlap parameter d_α allows to generate aggregates with high porosity ϕ.

C. Performance

In terms of performance, the BLOSSOM model being coded in MATLAB®, the generation of the 192 aggregates with $N_p = 200$ takes about 5 seconds on a machine equipped with an Intel® Core™ i9-12900KF processor at 3.19Ghz and 64GB of RAM. The generation of an aggregate of 5000 particles is of the order of a tenth of a second on the same machine. The parameters with the most influence on the performance of the model are the number of particles N_p and the displacement step $\Delta\rho$. Indeed, the larger $\Delta\rho$ is, the faster the aggregate will blossom.

V. Model fitting and validation

In this section, the method for fitting the BLOSSOM model parameters to real data is presented. For this purpose, an aggregate of quasi-spherical particles was 3D printed. The 3D morphological characteristics of this aggregate are well known, as they are contained in a reference STL file (Fig. 4). Then, 2D projection images of the aggregate were made using a morphogranulometer and then binarized (Fig. 4 & Fig. 5a). In order to adjust the model parameters to the actual data, an optimization process must be applied to a cost function. The cost function, defined later by equation (7), will allow to compare the 2D morphological characteristics of the synthetic aggregates generated by the BLOSSOM model to those of the 3D printed aggregate. To do this, the images from the morphogranulometer are used, and the necessary measurements are performed.

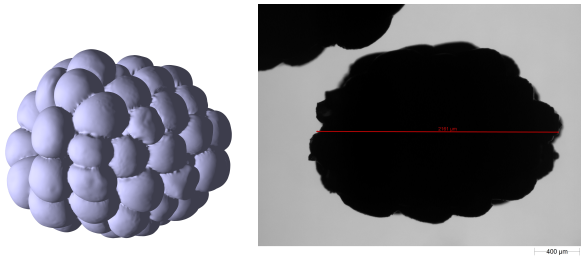

Fig. 4: Left: Visualization of the reference STL file containing the 3D structure of the aggregate to be 3D printed. Right: Raw image from the morphogranulometer.

Nevertheless, in order to work properly, the model requires two probability density functions. The following section presents a method to estimate f_θ by image analysis and makes a hypothesis about f_φ.

A. Computing f_θ and f_φ with image analysis

In a spherical coordinates system, a point in space is defined by three numbers:

$$\rho \in \mathbb{R}_+, \quad \varphi \in [-\pi;\pi] \quad \text{and} \quad \theta \in [-\pi/2;\pi/2]. \tag{5}$$

In order to simplify the problem, it is assumed that the aggregates to be characterized offer a certain cylindrical symmetry, as in the third example in Fig. 2. This immediately translates into the fact that the probability density function of φ is uniform, i.e.

$$\varphi \sim \mathbb{U}(-\pi, \pi) \tag{6}$$

where $\mathbb{U}$ is the continuous uniform distribution.

For the characterization of f_θ, a binary image of the aggregate to be characterized is used. The centroid of the shape is calculated (Fig. 5b) and the shape is split in two along a line parallel to the maximum Feret diameter passing through the centroid. A symmetry operation is performed on one of the two sub-images, and after the two parts are merged together

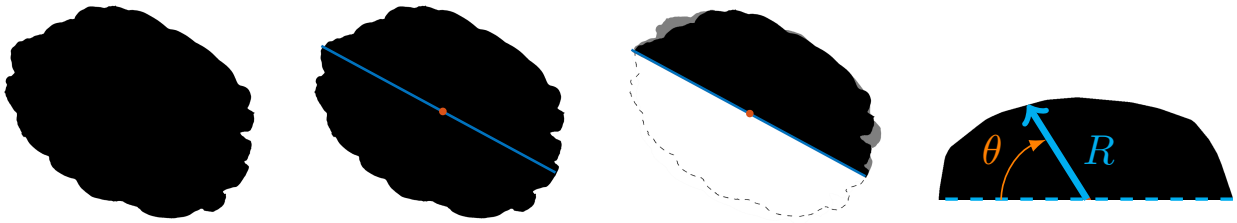

(a) (b) (c) (d)

Fig. 5: From left to right: Image from the morphogranulometer after binarization (5a), calculation of the centroid of the shape and alignment of the line in the direction of $F_{\max}$ (5b), merging of the two opposite halves (5c) and calculation of the probability density function f_θ (5d).

(Fig. 5c), the convex hull of the resulting shape is computed. For each angle $\theta \in [-\pi/2; \pi/2]$, the maximum length R between the centroid computed earlier and the shape boundary is calculated (Fig. 5d). Fig. 5 illustrates these different steps.

After computing the maximum distance R for several values of θ, an estimate of the probability density f_θ is calculated, as shown in Fig. 6.

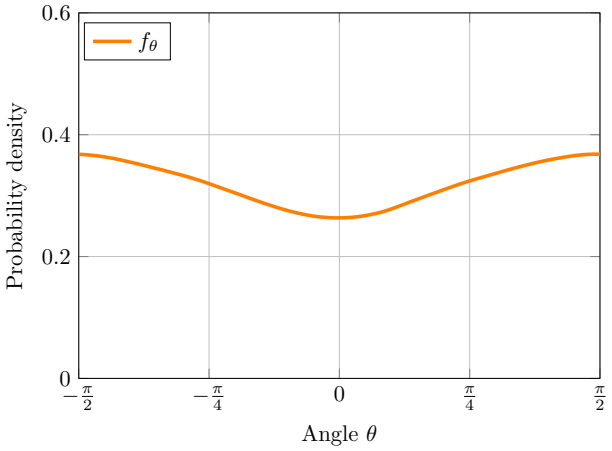

Fig. 6: Probability density function f_θ estimated from the aggregate projection image from the morphogranulometer in Fig. 5.

B. Cost function definition

Once the two probability density functions f_θ and f_φ are computed, the other 4 parameters of the model must be fitted to the real data. In order to do so, a cost function must be defined. The general idea is to generate multiple synthetic aggregates and compare their 2D morphological characteristics to those measured on the aggregate images from the morphogranulometer. Therefore, the cost function allows to quantify the differences between the measured morphological characteristics and is defined as follows.

$$F_{\text{cost}}(\omega) = 3\Delta(A_p)+3\Delta(P)+3\Delta(\Psi_{AR})+\Delta(F_{\max})+\Delta(F_{\min}) \quad (7)$$

with A_p the projected area, P the perimeter, Ψ_{AR} the aspect ratio, $F_{\max}$ (resp. $F_{\min}$) the maximum (resp. minimum) Feret diameter and $\omega = \{N_p, r, d_\alpha, \Delta\rho\}$ a set of 4 parameters of the model. The quantities Δx represent the relative errors between a characteristic x measured on an aggregate generated by the model with the set of parameters ω and the result of the measurement performed on an image from the morphogranulometer. Regarding the weights associated with each of the relative errors, they were determined empirically. In particular, the errors on the Feret diameters were added in order to better fit the distance step parameter $\Delta\rho$.

C. Model validation

The validation of the model consists in finding an optimal set of parameters $\widetilde{\omega}$ by minimizing the cost function F_{cost} and then comparing the 3D morphological characteristics of the aggregates generated by the BLOSSOM model with $\widetilde{\omega}$ (Fig. 7) to those of the 3D printed aggregate, whose 3D morphological characteristics are known thanks to the STL file. The optimization is performed using a simulated annealing algorithm. At each iteration, 192 aggregates are generated from the same set of parameters and the morphological characteristics measured are being averaged before being compared to those of the real images.

The results of the optimization process are presented in Table II. It is noticeable that all the characteristics measured on the synthetic aggregates are extremely close to those of the reference aggregate, with the single exception of the surface area S. Indeed, the relative errors on the 2D characteristics are

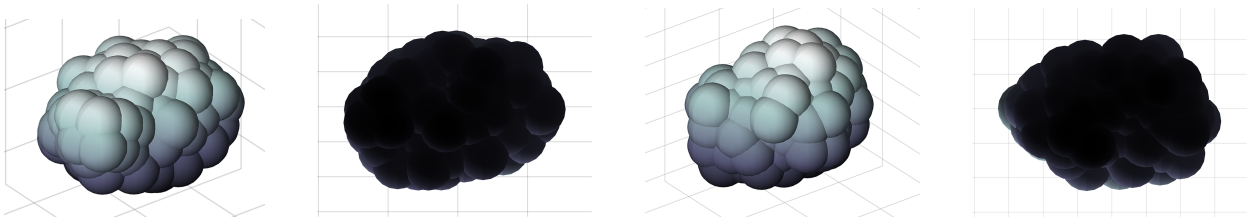

Fig. 7: Examples of aggregates generated by the BLOSSOM model using the optimal set of parameters $\widetilde{\omega}$ with their respective projections. The direction of projection is always determined by the vector $\vec{n} = (1, 0, 0)$, whether in Cartesian or spherical coordinates, in order to remain consistent with the way the distribution f_θ was estimated.

TABLE II: Comparison of 2D and 3D morphological properties measured on the 3D printed reference aggregate and those proposed by the BLOSSOM model from the optimal set of parameters $\widetilde{\omega}$, averaged over 192 realizations.

	2D			**3D**							
Properties	A_p (mm^2)	P (mm)	Ψ_{AR}	V (mm^3)	V_c (mm^3)	S (mm^2)	SLD	ESD (mm)	PAL_1 (mm)	PAL_2 (mm)	PAL_3 (mm)
Ground truth	2.73	6.75	0.71	2.34	2.76	11.25	0.84	1.65	1.98	1.54	1.52
BLOSSOM model	2.73	6.73	0.71	2.32	2.75	10.19	0.84	1.65	2.06	1.56	1.55
Error (%)	0.1%	0.2%	0.3%	0.6%	0.1%	9.4%	0.3%	0.2%	4.1%	1.6%	2.2%

less than 1%, and the errors on the 3D characteristics are also less than 2% in most cases. The specific case of the higher relative error on the surface area S can probably be partly explained by the fact that the 3D structure contained in the STL file is not convex and presents a strong concavity at one of the tips of the aggregate. This leads to an increase in the surface area of the reference aggregate, which remains difficult to quantify, without being apparent on the 2D projections from the morphogranulometer.

Another reason, more subtle, can be related to the errors made on the PAL. Indeed, one can see that PAL_2 and PAL_3 are not identical, which partially invalidates the initial hypothesis of a cylindrical symmetry of the aggregate. Therefore, relatively larger errors are made on PAL_2 and PAL_3 and, since the surface area S of a flattened cylinder is larger than the one of a perfect cylinder, it seems natural that this characteristic is again slightly underestimated.

D. Comparison with other methods

Comparing the performance of the proposed method with others is difficult. Indeed, a first reason is the fact that the estimation of the 3D morphological characteristics of an aggregate is usually done from several images, with multiple cameras [13] or a mobile one [14] whereas our approach uses only one single image.

Moreover, one of the main reasons why the comparison is difficult is that the ground truth is usually unknown. Under these conditions, it is impossible to estimate the error on the measured characteristics. The proposed approach allows this only because a calibrated 3D printed aggregate is available.

Nevertheless, [14] propose an estimation of the relative error using a method based on a 3D reconstruction from a mobile camera for crystalline aggregates. The relative errors are estimated for a sphere, a cylinder and an hexagonal prism and are in the range of 1% to 3.5%, both for the volume V and the surface area S.

Hence, even an approach based on multiple images of rather simple objects does not provide a better estimate of the volume V than the BLOSSOM model does. As for the surface area S, the relative error made by the method proposed in this paper remains higher, but it is to be put in perspective with the shape of the aggregate studied, which is far more complex, and the nature of the aggregate, which is not a crystal, but made of spherical primary particles.

VI. Conclusion

The results presented in the previous section show that it is possible to validate the proposed method on a specific case, with very good results on all the measured morphological characteristics (2D and 3D), except for the surface area, although some explanations have been proposed to explain this discrepancy. In particular, the BLOSSOM model was shown to be flexible enough to be able to generate spherical particle aggregates with the same morphological characteristics as the 3D printed aggregate from a reference STL file.

That being said, there are still many areas for improvement. Indeed, the error on the surface area can probably be reduced by giving up the assumption of a cylindrical symmetry. Nevertheless, this strong assumption is mainly due to the fact that only a single 2D projection is used, which tremendously reduces the knowledge of the aggregate to be characterized. Indeed, the use of multiple uncalibrated projections is under study and will be the focus of future work.

Moreover, one of the next steps is the application of the method to the characterization of real aggregates, with images acquired directly in-situ in the industrial reactor. The enhancement of the model, through the use of non-spherical particles or of different size is also an interesting idea, especially since the particles used to print the 3D aggregate are themselves neither perfectly spherical, nor of identical size.

Acknowledgment

The author(s) acknowledge(s) the support of the French Agence Nationale de la Recherche (ANR), under grant ANR-20-CE07-0025 (project MORPHING).

References

[1] S. Tang, C. M. McFarlane, G. C. Paul, and C. R. Thomas, "Characterising latex particles and fractal aggregates using image analysis," *Colloid and Polymer Science*, vol. 277, no. 4, pp. 325–333, Apr 1999.

[2] B. Sung and L. Abelmann, "Agglomeration structure of superparamagnetic nanoparticles in a nematic liquid crystal medium: Image analysis datasets based on cryo-electron microscopy and polarised optical microscopy techniques," *Data in Brief*, vol. 34, p. 106716, 2021.

[3] E. M. Alander, M. S. Uusi-Penttilä, and Åke C Rasmuson, "Characterization of paracetamol agglomerates by image analysis and strength measurement," *Powder Technology*, vol. 130, no. 1, pp. 298–306, 2003.

[4] Y. Huo, T. Liu, H. Liu, C. Y. Ma, and X. Z. Wang, "In-situ crystal morphology identification using imaging analysis with application to the l-glutamic acid crystallization," *Chemical Engineering Science*, vol. 148, pp. 126–139, 2016.

[5] N. Faria, M. Pons, S. Feyo de Azevedo, F. Rocha, and H. Vivier, "Quantification of the morphology of sucrose crystals by image analysis," *Powder Technology*, vol. 133, no. 1, pp. 54–67, 2003.

[6] C. Turchiuli and E. Castillo-Castaneda, "Agglomerates structure characterization using 3d-image reconstruction," *Particle & Particle Systems Characterization*, vol. 26, no. 1-2, pp. 25–33, 2009.

[7] F. Z. Vissotto, R. C. Giarola, L. C. Jorge, G. T. Makita, G. M. B. Q. Cardozo, M. I. Rodrigues, and F. C. Menegalli, "Morphological characterization with image analysis of cocoa beverage powder agglomerated with steam," *Food Science and Technology*, vol. 34, no. Food Sci. Technol, 2014 34(4), Oct 2014.

[8] I. Atalar and F. Yazici, "Effect of different binders on reconstitution behaviors and physical, structural, and

morphological properties of fluidized bed agglomerated yoghurt powder," *Drying Technology*, vol. 37, no. 13, pp. 1656–1664, 2019.

[9] R. Pashminehazar, A. Kharaghani, and E. Tsotsas, "Three dimensional characterization of morphology and internal structure of soft material agglomerates produced in spray fluidized bed by x-ray tomography," *Powder Technology*, vol. 300, pp. 46–60, 2016, 7th International Granulation Workshop 2015: Granulation across the length scales.

[10] C. Jin, F. Zou, X. Yang, and Z. You, "3d quantification for aggregate morphology using surface discretization based on solid modeling," *Journal of Materials in Civil Engineering*, vol. 31, no. 7, p. 04019123, 2019.

[11] M. Pons, V. Plagnieux, H. Vivier, and D. Audet, "Comparison of methods for the characterisation by image analysis of crystalline agglomerates: The case of gibbsite," *Powder Technology*, vol. 157, no. 1, pp. 57–66, 2005, 4th French Meeting on Powder Science and Technology.

[12] A.-F. Blandin, A. Rivoire, D. Mangin, J.-P. Klein, and J.-M. Bossoutrot, "Using in situ image analysis to study the kinetics of agglomeration in suspension," *Particle & Particle Systems Characterization*, vol. 17, no. 1, pp. 16–20, 2000.

[13] Y. Huo, T. Liu, X. Z. Wang, C. Y. Ma, and X. Ni, "Online detection of particle agglomeration during solution crystallization by microscopic double-view image analysis," *Industrial & Engineering Chemistry Research*, vol. 56, no. 39, pp. 11 257–11 269, Oct 2017.

[14] J. P. Zavala De Paz, C. Isaza Bohorques, E. Anaya Rivera, and E. Castillo Castaneda, "Morphological characterization of agglomerated particles by 3d reconstruction," *IEEE Latin America Transactions*, vol. 14, no. 7, pp. 3117–3123, 2016.

[15] Z. M. Lu, L. Zhang, D. M. Fan, N. M. Yao, and C. X. Zhang, "Crystal texture recognition system based on image analysis for the analysis of agglomerates," *Chemometrics and Intelligent Laboratory Systems*, vol. 200, p. 103985, 2020.

[16] M. Frei and F. E. Kruis, "Fully automated primary particle size analysis of agglomerates on transmission electron microscopy images via artificial neural networks," *Powder Technology*, vol. 332, pp. 120–130, 2018.

[17] P. Monchot, L. Coquelin, K. Guerroudj, N. Feltin, A. Delvallée, L. Crouzier, and N. Fischer, "Deep learning based instance segmentation of titanium dioxide particles in the form of agglomerates in scanning electron microscopy," *Nanomaterials*, vol. 11, no. 4, 2021.

[18] A. Mehle, B. Likar, and D. Tomaževič, "In-line recognition of agglomerated pharmaceutical pellets with density-based clustering and convolutional neural network," in *2017 Fifteenth IAPR International Conference on Machine Vision Applications (MVA)*, 2017, pp. 9–12.

[19] B. Rühle, J. F. Krumrey, and V.-D. Hodoroaba, "Workflow towards automated segmentation of agglomerated, non-spherical particles from electron microscopy images using artificial neural networks," *Scientific Reports*, vol. 11, no. 1, p. 4942, Mar. 2021.

[20] F. Einar Kruis, J. van Denderen, H. Buurman, and B. Scarlett, "Characterization of agglomerated and aggregated aerosol particles using image analysis," *Particle & Particle Systems Characterization*, vol. 11, no. 6, pp. 426–435, 1994.

[21] L. Theodon, T. Eremina, K. Dia, F. Lamadie, J.-C. Pinoli, and J. Debayle, "Estimating the parameters of a stochastic geometrical model for multiphase flow images using local measures," *Image Analysis & Stereology*, vol. 40, no. 3, pp. 115–125, 2021.

[22] L. Théodon, J. Laurencin, M. Hubert, P. Cloetens, and J. Debayle, "A stochastic geometrical 3d model for time evolution simulation of microstructures in soc-electrodes," *Computational Materials Science*, vol. 212, p. 111568, 2022.

[23] L. Theodon, C. Coufort-Saudejaud, and J. Debayle, "Grape: A stochastic geometrical 3d model for aggregates of particles with tunable 2d morphological projected properties," *Image Analysis & Stereology*, vol. 42, no. 1, pp. 1–16, 2023.

[24] S. Wang, H. Liu, C. Yang, and Y. Li, "Experimental investigation on the microstructure of fluidized nanoparticle agglomerates by tem image analysis," *The Canadian Journal of Chemical Engineering*, vol. 99, no. 5, pp. 1125–1136, 2021.

[25] K. V. Mardia and P. J. Zemroch, "Algorithm as 86: The von mises distribution function," *Journal of the Royal Statistical Society. Series C (Applied Statistics)*, vol. 24, no. 2, pp. 268–272, 1975.